BJR

https://doi.org/10.1259/bjr.20200677

Received: 04 June 2020 | Revised: 06 October 2020 | Accepted: 08 October 2020

Cite this article as:
Steuwe A, Weber M, Bethge OT, Rademacher C, Boschheidgen M, Sawicki LM, et al. Influence of a novel deep-learning based reconstruction software on the objective and subjective image quality in low-dose abdominal computed tomography. *Br J Radiol* 2020; **94**: 20200677.

FULL PAPER

Influence of a novel deep-learning based reconstruction software on the objective and subjective image quality in low-dose abdominal computed tomography

ANDREA STEUWE, PhD, MARIE WEBER, OLIVER THOMAS BETHGE, Dipl Ing, CHRISTIN RADEMACHER, MD, MATTHIAS BOSCHHEIDGEN, MD, LINO MORRIS SAWICKI, MD, PhD, GERALD ANTOCH, MD, PhD and JOEL AISSA, MD, PhD

Department of Diagnostic and Interventional Radiology, University Dusseldorf, Medical Faculty, Dusseldorf, Germany

Address correspondence to: Dr Andrea Steuwe
E-mail: *andrea.steuwe@med.uni-duesseldorf.de*

Objectives: Modern reconstruction and post-processing software aims at reducing image noise in CT images, potentially allowing for a reduction of the employed radiation exposure. This study aimed at assessing the influence of a novel deep-learning based software on the subjective and objective image quality compared to two traditional methods [filtered back-projection (FBP), iterative reconstruction (IR)].

Methods: In this institutional review board-approved retrospective study, abdominal low-dose CT images of 27 patients (mean age 38 ± 12 years, volumetric CT dose index 2.9 ± 1.8 mGy) were reconstructed with IR, FBP and, furthermore, post-processed using a novel software. For the three reconstructions, qualitative and quantitative image quality was evaluated by means of CT numbers, noise, signal-to-noise ratio (SNR), and contrast-to-noise ratio (CNR) in six different ROIs. Additionally, the reconstructions were compared using SNR, peak SNR, root mean square error and mean absolute error to assess structural differences.

Results: On average, CT numbers varied within 1 Hounsfield unit (HU) for the three assessed methods in the assessed ROIs. In soft tissue, image noise was up to 42% lower compared to FBP and up to 27% lower to IR when applying the novel software. Consequently, SNR and CNR were highest with the novel software. For both IR and the novel software, subjective image quality was equal but higher than the image quality of FBP-images.

Conclusion: The assessed software reduces image noise while maintaining image information, even in comparison to IR, allowing for a potential dose reduction of approximately 20% in abdominal CT imaging.

Advances in knowledge: The assessed software reduces image noise by up to 27% compared to IR and 48% compared to FBP while maintaining the image information.

The reduced image noise allows for a potential dose reduction of approximately 20% in abdominal imaging.

INTRODUCTION

The radiation exposure in CT with its concomitant risk of inducing cancerous diseases motivates the need for dose reduction and optimization of scan protocols.[1,2] Advancements for dose reduction in CT are based on hardware (*i.e.* increasing detector sensitivity), on scan protocol settings (reduction of tube potential and/or tube current–time product) and on software (automatic exposure control, reconstruction techniques and post-processing methods).[3] For scan protocol settings with reduced radiation exposure to the patient, the image quality deteriorates since the image detector receives less signal due to the decreased radiation exposure. Depending on the underlying image reconstruction method, the effect of dose reduction on the processed image varies.

Traditional filtered back-projection (FBP) is a computationally simple technique, where the measured raw data from projection space are transformed to processed image space. FBP is a fast and robust technique, requires limited computational power and is applicable in clinical routine.[4] However, the reconstructed images can appear noisy if low dose techniques are employed or only insufficient projection data are available, causing a lower visibility of low-contrast structures and image artifacts are often significant.[4–6]

Iterative reconstruction (IR) techniques provide a lower amount of image noise and improve visibility of low-contrast structures.[7,8] Due to the reduced image noise, IR allows to decrease the applied radiation dose in CT while maintaining image quality.[6,9] However, reconstruction time is considerably longer than FBP. Another side-effect of IR is the altered image appearance: Images often look artificially smooth (plastic-like) due to altered signal values (pixel data).[4,5,10,11]

In the last years, more and more software has been developed for reduction of image noise in CT. In literature, some of the software has been described previously.[12–15] The commercial product PixelShine (AlgoMedica, Inc., Sunnyvale, CA) is a novel software based on an artificial neural network technique (deep learning) that reduces image noise in CT.[16] Ultra-large amounts of high-dose and low-dose data have been used for training of the software.[17] After training, the software makes use of filtered back-projected CT images for post-processing. In contrast, the techniques FBP or IR use projection data (raw data) as input for image reconstruction instead if image data. The vendor claims that the software decreases image noise without altering the image information or rendering the image appearance to blotchy or plastic-like impression. Up to now, only one full paper covers the application and value of PixelShine in human imaging (low-dose pelvic arterial phase images),[17] whereas just two others cover phantom studies.[16,18] Further studies need to be performed to evaluate the software in other clinical settings.

When performing low-dose CT imaging of the abdomen, considerable image noise occurs especially for patients with high body mass indices or large effective diameters due to increased absorption of X-rays in the abdominal (fat) tissue. In the institution, where this study is performed, low-dose abdominal imaging is performed in cases of urinary stone diagnostics or in case of suspected drug body packing as part of a criminal investigation. These indications allow for low-dose imaging since urinary stones or body packs are usually high-contrast materials, however, only if IR for noise suppression is applied.[19] The drawback of IR images is the increased blotchiness of images with decreasing noise level. Therefore, the aim of the study was to evaluate whether PixelShine might be an alternative to IR or even lead to a superior image quality than IR in human low-dose abdominal imaging. For this purpose, the study evaluates and compares the subjective and objective image quality of images reconstructed with FBP, IR and PixelShine in low-dose abdominal CT examinations.

Table 1. Patient and imaging characteristics

Parameter	Mean	±	SD
Age (years)	37.6	±	11.5
Effective TCTP (mAs)	148.0	±	93.9
$CTDI_{vol}$ (mGy)	2.9	±	1.8
DLP (mGy·cm)	137.6	±	88.6
Effective dose (mSv)	2.24	±	1.44
Scan length (cm)	46.5	±	4.1
Diameter lateral (mm)	349.6	±	57.5
Diameter ap (mm)	246.1	±	55.6
Effective diameter (mm)	293.0	±	55.6

AP, anteroposterior; $CTDI_{vol}$, volumetric computed tomography dose index; DLP, dose–length product; SD, standard deviation;effective TCTP, effective tube current–time product.

METHODS AND MATERIALS

In this IRB-approved retrospective study, 27 patients (19 male, 8 female) receiving a low-dose abdominal CT scan between November 2014 and February 2016 were included. The examined patients were suspected of body packing, therefore, a low-dose protocol was employed. A full-dose abdominal CT scan was not performed in these patients.

Image acquisition and post-processing

CT protocol parameters were as follows: tube potential 80 kV_p, reference tube current–time product 160 mAs, 0.5 s rotation time, 0.6 mm collimation, pitch 0.6. Images were acquired on a Somatom Definition Flash CT scanner (Siemens Healthineers, Forchheim, Germany). The scan range covered the diaphragm to the ischium.

Raw CT data were reconstructed and post-processed as follows:

(1) FBP: 2.0 mm slice thickness, kernel B30f, increment 1.7 mm.
(2) PS: FBP (see reconstruction 1) with PixelShine (PS), settings: P214A8S.
(3) IR: 2.0 mm slice thickness, kernel I30f, level 3, increment 1.7 mm (SAFIRE, Siemens Healthineers, Fochheim, Germany).

SAFIRE (sinogram-affirmed iterative reconstruction) utilizes both raw data (projection data) and image data iterations with up to five strength levels to control for image impression and noise reduction.[4] In SAFIRE, the initial reconstruction is performed using FBP images, after which two different correction loops are implemented, during which noise is reduced.

PixelShine v. 1.2.104's adaptive processing mode was employed with the following reconstruction parameters for abdominal imaging: sharpening level P2 (a linear filter applied before the noise reduction process), target noise level 14 (based on Hounsfield unit, HU), maximum processing strength A8 (55% noise reduction, equivalent dose or thickness x4.9), and smoothing type S (soft kernel). In the adaptive processing mode, the software estimates noise levels in the original images and adaptively applies appropriate processing strength to obtain the target noise level images. The vendor (AlgoMedica) specified the parameters for the combination of the CT scanner type and abdominal imaging (soft tissue). Since PixelShine is a commercial product, we were not able to obtain information related to the deep-learning structure, training and operating principle of the software.

Objective image analysis

For all patients and data sets, circular regions-of-interest (ROIs) ($r \approx 10$ mm) were drawn in the liver, spleen, aorta, paravertebral muscle, fat and in the background (air) using the software

Table 2. Mean CT number ± SD (top) and mean noise ± SD (bottom) of the regions-of-interest measured in the background and the five body tissues

	Liver	Muscle	Spleen	Air	Fat	Aorta
CT number (HU)						
FBP	49.5 ± 14.7	52.9 ± 10.7	36.7 ± 10.1	−992.1 ± 10.8	−126.8 ± 12.6	45.3 ± 9.4
PS	49.4 ± 14.8	52.2 ± 10.6	36.4 ± 10.2	−992.5 ± 10.6	−126.6 ± 12.3	44.2 ± 9.1
IR	49.6 ± 14.8	52.9 ± 10.5	36.8 ± 10.1	−992.8 ± 11.2	−126.7 ± 12.6	45.4 ± 9.1
Noise (HU)						
FBP	45.9 ± 9.6	42.7 ± 7.6	43.9 ± 9.3	22.2 ± 12.4	35.3 ± 5.6	36.6 ± 6.7
PS	26.8 ± 7.5	24.0 ± 6.2	25.1 ± 6.6	10.0 ± 13.4	18.0 ± 4.9	24.8 ± 5.1
IR	31.7 ± 6.7	29.6 ± 5.4	30.5 ± 6.3	16.9 ± 13.0	24.9 ± 4.2	26.6 ± 5.0

FBP: Reconstruction with filtered back-projection, HU: Hounsfield unit, IR: Iterative reconstructed images; PS: PixelShine employed on FBP-images;SD, standard deviation.

ImageJ, v. 1.52 n (National Institutes of Health, USA). For each patient, ROIs were drawn in exactly the same position for each reconstruction method. Mean CT number and standard deviation (noise) were determined in each ROI.

Contrast-to-noise ratio (CNR) and signal-to-noise (SNR_{ROI}) ratio were calculated using the following formulas:

$$CNR = \frac{CT_{tissue} - CT_{fat}}{SD_{fat}}$$

for the muscle, spleen, liver and the aorta and

$$SNR_{ROI} = \frac{CT_{ROI}}{SD_{ROI}}$$

for all ROIs with CT_{tissue} or CT_{ROI} as CT number of a certain ROI and SD_{fat} or SD_{ROI} for the standard value of a certain ROI.

Furthermore, for the total image data sets, the SNR (in decibel, dB), peak SNR (PSNR, in dB), root mean square error (RMSE)

Table 3. Absolute and relative difference of CT numbers ± SD (top) and noise ± SD (bottom) for the different post-processing types

	Liver	Muscle	Spleen	Air	Fat	Aorta
CT number						
Absolute difference (HU)						
PS *vs* FBP	−0.1 ± 0.5	−0.7 ± 0.7	−0.3 ± 0.7	−0.4 ± 0.7	0.2 ± 0.7	−1.1 ± 0.9
PS *vs* IR	−0.2 ± 0.5	−0.7 ± 0.5	−0.3 ± 0.6	0.4 ± 1.1	0.1 ± 0.7	−1.2 ± 1.1
IR *vs* FBP	0.0 ± 0.4	0.0 ± 0.4	0.1 ± 0.4	−0.7 ± 0.8	0.1 ± 0.6	0.1 ± 0.7
Relative difference (%)						
PS *vs* FBP	−0.4 ± 1.8	−1.2 ± 1.4	−1.1 ± 4.3	0.0 ± 0.1	−0.1 ± 0.6	−2.4 ± 1.9
PS *vs* IR	−0.2 ± 1.8	−1.4 ± 1.2	−1.3 ± 4.3	0.0 ± 0.1	−0.1 ± 0.5	2.8 ± 2.5
IR *vs* FBP	−0.1 ± 2.2	0.2 ± 1.1	0.2 ± 1.4	0.1 ± 0.1	−0.1 ± 0.5	0.4 ± 1.8
Noise						
Absolute difference (HU)						
PS *vs* FBP	−19.1 ± 7.2	−18.7 ± 7.0	−18.8 ± 7.1	−12.2 ± 3.8	−17.3 ± 6.4	−11.7 ± 5.1
PS *vs* IR	−4.9 ± 5.0	−5.6 ± 5.3	−5.4 ± 4.8	−6.9 ± 2.3	−6.9 ± 4.9	−1.8 ± 3.4
IR *vs* FBP	−14.2 ± 3.3	−13.1 ± 2.6	−13.4 ± 3.4	−5.3 ± 1.7	−10.4 ± 2.1	−9.9 ± 2.4
Relative difference (%)						
PS *vs* FBP	−41.2 ± 12.5	−43.3 ± 13.0	−42.4 ± 11.9	−62.5 ± 18.8	−48.2 ± 14.8	−31.4 ± 12.0
PS *vs* IR	−15.3 ± 16.0	−18.4 ± 17.4	−17.4 ± 15.5	−49.7 ± 18.4	−27.1 ± 18.7	−6.1 ± 14.3
IR *vs* FBP	−30.9 ± 2.7	−30.7 ± 2.5	−30.4 ± 2.9	−27.6 ± 8.4	−29.4 ± 3.9	−27.1 ± 4.1

FBP: reconstruction with filtered back-projection, HU: Hounsfield unit, IR: iterative reconstructed images; PS: PixelShine employed on FBP-images;SD, standard deviation.

Figure 1. Axial slice through the liver, reconstructed using (a) FBP) (b) FBP with PS and (c) using IR. Image viewer settings (window 310/level 45). FBP, filtered back-projection; IR, iterative reconstruction; PS, PixelShine.

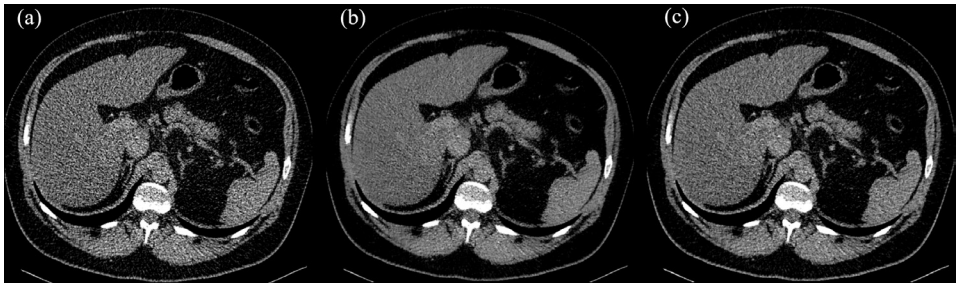

and mean absolute error (MAE) were calculated with the FBP image data set as reference images, using the plugin "SNR" for the software ImageJ, v. 1.52n (National Institutes of Health, USA).[20] The calculation for each quantity is performed image-wise. The measures were then averaged over the all images for each patient and reconstruction.

Noise-images were acquired using the software ImageJ, v. 1.52n (National Institutes of Health, USA). ImageJ offers the possibility to subtract images pixelwise. This was performed to calculate subtraction images from the three processed image data sets.

Subjective image analysis

Two radiologists (10 and 2 years of experience in radiology) independently rated image quality using a 5-point Likert scale [(1) excellent image quality, (2) good image quality, (3) moderate image quality, (4) poor image quality, (5) non-diagnostic image quality].

Statistical analysis

For both the objective and the subjective image quality, the following comparisons were obtained:

(1) Comparison PS with FBP
(2) Comparison PS with IR
(3) Comparison IR with FBP

For all 6 ROIs, the CT numbers and image noise (12 data sets per reconstruction type) were compared and evaluated.

Commercially available software (Microsoft Excel 2016, Redmond, WA; SPSS, 26.0, Inc., Chicago, IL) was used to perform statistical analysis. Continuous data are expressed as mean ± SD. Differences in objective and subjective image quality among the reconstruction methods were calculated by means of a Bonferroni-corrected Wilcoxon-test using a significance level dependent on the number of evaluated tests (ROIs and comparisons). Inter-reader reliability was determined using a Fleiss κ with chance-correction according to Brennan and Prediger.[21]

RESULTS

Patient collective and effective dose

In this study, 27 patients (19 male, 8 female) with a mean age of 38 ± 12 years (range 20–58) and an average effective abdominal diameter of 29.3 cm (measured on central reconstructed CT slice ($\sqrt{d_{lat} * d_{ap}}$) were included (c.f. Table 1). A $CTDI_{vol}$ of 2.9 ± 1.8 mGy and a DLP of 137.6 ± 88.6 mGy·cm with an effective tube current–time product of 148.0 ± 93.9 mAs at 80 kV_p resulted in an average effective dose of 2.24 ± 1.44 mSv (conversion factor of 0.0163 mSv/(mGy·cm) for the abdomen[22]).

Objective image quality

CT number

The average CT numbers obtained by the three reconstruction methods for the evaluated ROI positions were within ±1 HU (absolute difference) or 3% (relative difference), see Tables 2 and 3. There were significant differences between CT numbers in the muscle and aorta (PS *vs* FBP and PS *vs* IR) and in the air (IR *vs*

Table 4. Results of Bonferroni-corrected Wilcoxon test for the CT number and regions-of-interest measured in the background and the five body tissues

	Liver	Muscle	Spleen	Air	Fat	Aorta
CT number						
PS *vs* FBP	0.179	0.000	0.032	0.007	0.178	0.000
PS *vs* IR	0.088	0.000	0.007	0.058	0.588	0.000
IR *vs* FBP	0.492	0.879	0.568	0.000	0.525	0.486
Noise						
PS *vs* FBP	0.000	0.000	0.000	0.000	0.000	0.000
PS *vs* IR	0.000	0.000	0.000	0.000	0.000	0.000
IR *vs* FBP	0.000	0.000	0.000	0.000	0.000	0.000

FBP: reconstruction with filtered back-projection, IR: iterative reconstructed images; PS: PixelShine employed on FBP-images.
A *p*-value of 0.0028 was considered statistically significant (3 × 6 comparisons → $p = 0.5/18 = 0.0028$).

Figure 2. Zoomed view of an axial slice through the liver and kidneys (left column) and in the air (right column), reconstructed using FBP (top row), FBP with PS (middle row) and using IR (bottom row). Image viewer settings (window 310/level 45). FBP, filtered back-projection; IR, iterative reconstruction; PS, PixelShine.

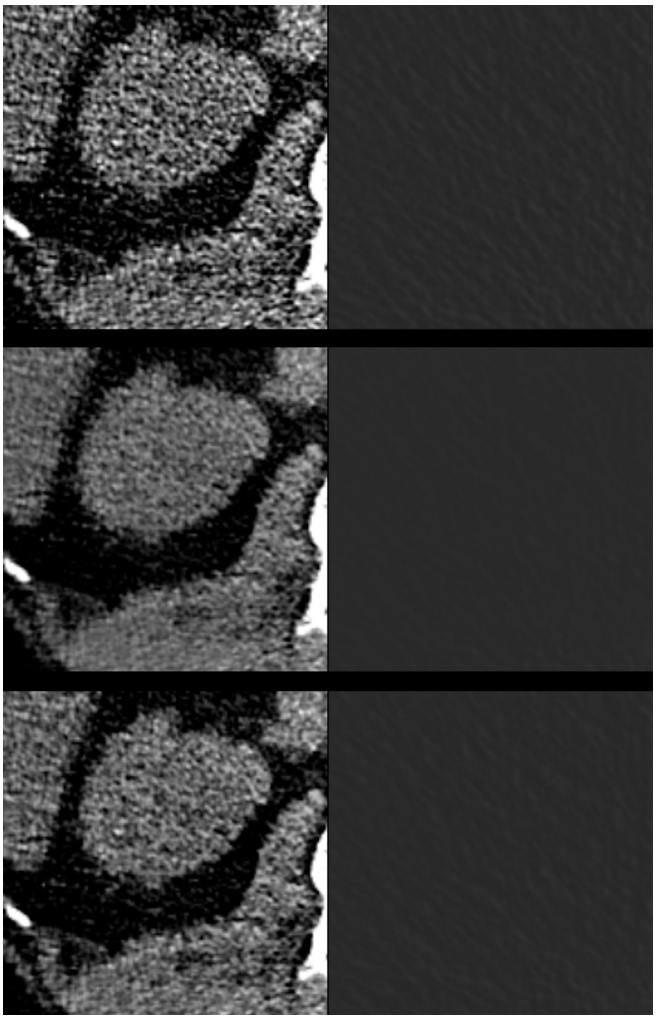

FBP), although the maximum difference in CT numbers was only 3 HU, see Tables 2–4.

Image noise

Image noise was lowest when employing PixelShine, and highest when using FBP, see Tables 2 and 3. See Figure 1 for an abdominal slice and Figure 2 for zoomed sections of the slice, reconstructed with the three evaluated methods. Between PS and FBP, the noise in the evaluated ROIs is reduced by 12–19 HU (air: average reduction of 12 HU or 63%, tissues: reduction of approximately 18 HU or 40–48%, aorta: reduction of 12 HU or 31%)), see Tables 2–4. Comparing PS and IR, the image noise was lower in PS reconstructions by 2–7 HU (muscle, liver, spleen −15–18%, air-50%, fat −27%, aorta −6%). Image noise was approximately 30% lower in all evaluated ROIs when employing IR compared to FBP. Significant differences were visible for all evaluated ROI positions and reconstruction methods, see Table 4.

SNR in ROIs

The absolute value of the SNR was highest (Table 5) for images reconstructed with PS and lowest for FBP images. Differences among the reconstruction methods were statistically significant for all evaluated ROIs ($p < 0.001$).

CNR in ROIs

Between the four evaluated ROIs, CNR was highest for the liver and muscle (Table 5). Between the three evaluated reconstruction techniques, CNR was highest when using PS, due to the low image noise (see last section), increasing by about 40% compared to IR images and 90% compared to FBP. Differences among the reconstruction methods were statistically significant for all evaluated ROIs ($p < 0.001$).

SNR, PSNR, RMSE, MAE in image data sets

Comparing PS and IR image sets to the corresponding FBP image sets, SNR and PSNR were higher when comparing IR and FBP data sets with PS and FBP images ($SNR_{IR\text{-}FBP}$ 35.4 ± 1.4 dB *vs* $SNR_{PS\text{-}FBP}$ 33.6 ± 2.7 dB and $PSNR_{IR\text{-}FBP}$ to 43.2 ± 1.5 dB *vs* $PSNR_{PS\text{-}FBP}$ 41.4 ± 2.8 dB). The RMSE and MAE were lower when comparing IR and FBP data sets with PS and FBP data sets ($RMSE_{IR\text{-}FBP}$ 11.7 ± 1.4 *vs*

Table 5. SNR ± SD (top) and CNR ± SD (top), with respect to fat ROI

	Liver	Muscle	Spleen	Air	Fat	Aorta
SNR						
FBP	1.2 ± 0.5	1.3 ± 0.4	0.9 ± 0.4	−51.3 ± 13.9	−3.7 ± 0.7	1.3 ± 0.4
PS	2.0 ± 1.0	2.3 ± 0.9	1.6 ± 0.7	−168.7 ± 74.7	−7.7 ± 2.8	1.9 ± 0.8
IR	1.7 ± 0.7	1.9 ± 0.6	1.3 ± 0.5	−73.0 ± 22.2	−5.2 ± 1.0	1.8 ± 0.6
CNR						
FBP	5.1 ± 1.1	5.2 ± 1.0	4.7 ± 0.9			5.0 ± 0.9
PS	10.6 ± 3.6	10.7 ± 3.3	9.8 ± 3.0			10.4 ± 3.9
IR	7.3 ± 1.5	7.4 ± 1.4	6.7 ± 1.2			7.1 ± 1.3

CNR: contrast-to-noise ratio, FBP: reconstruction with filtered back-projection, IR: iterative reconstructed images; PS: PixelShine employed on FBP-images, ROI: region of interest,SD, standard deviation; SNR: signal-to-noise ratio.
Differences between reconstruction methods for SNR were significant ($p < 0.001$) for all ROIs except for the aorta (differences between IR and PS: $p = 0.155$). Differences between reconstruction methods for CNR were significant ($p < 0.001$) for all ROIs.

Figure 3. Rated image quality with standard deviation for the individual reader and both readers combined and κ value for intra-observer reliability. The image quality of PS- and IR-images sets were rated significantly higher than the image quality of FBP images ($p < 0.001$ for PS *vs* FBP and IR *vs* FBP, $p = 0.876$ for PS *vs* IR, significant differences marked with an asterisk). FBP, filtered back-projection; IR, iterative reconstruction; PS, PixelShine.

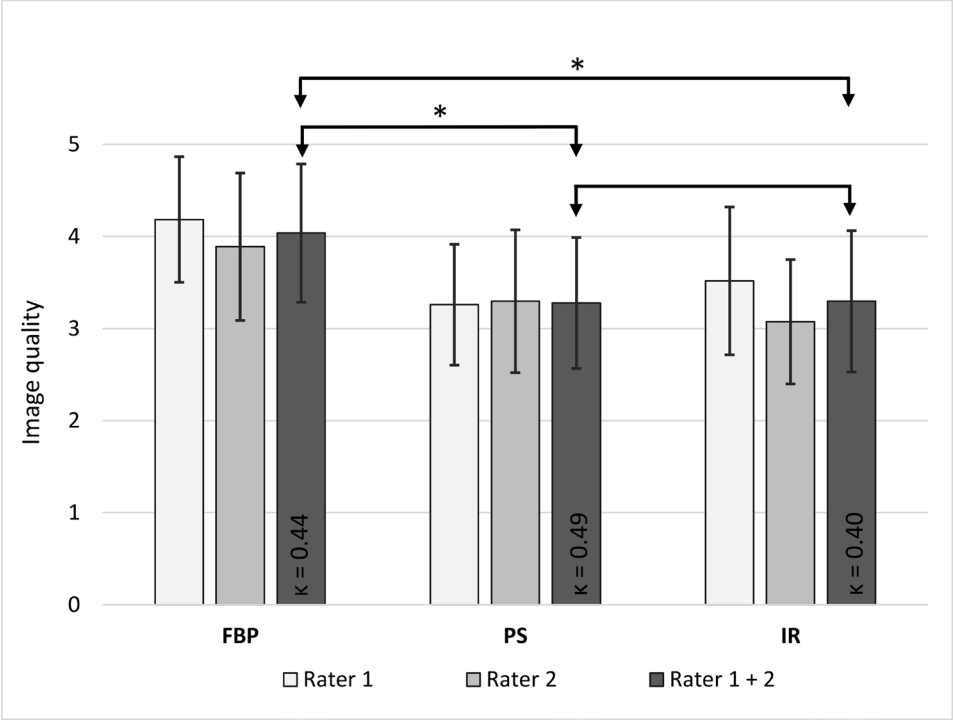

$RMSE_{PS\text{-}FBP}$ 15.1 ± 4.0 and $MAE_{IR\text{-}FBP}$ 8.3 ± 1.2 *vs* $MAE_{PS\text{-}FBP}$ 11.8 ± 3.0).

Subjective image quality

The image quality of the abdominal CT reconstructions was moderate to poor, since a low-dose protocol was employed (Figures 1 and 3). However, the image quality was sufficient for the detection of foreign materials. For the two raters, inter-reader reliability was fair to moderate (κ = 0.40–0.49). Applying solely FBP, the image quality was poor (4.0 ± 0.8), whereas it was moderate when applying PS (3.3 ± 0.7) or IR (3.3 ± 0.8). There was a significant difference in image quality between PS- and FBP-reconstructions and between IR- and FBP-reconstructions ($p < 0.001$, Figure 3). No significant difference in image quality was noted between PS- and IR-reconstructions although the visual impression differed ($p = 0.876$, Figures 1 and 2). As visible in Figures 1 and 2, the liver appears considerably noisier in FBP images compared to IR- or PS-processed images. The PS-processed images seem to be more homogeneous and smoother in each structure, removing little coarseness. With the increased homogeneity in the organs, IR- and PS-processed images appear less contrasty, compared to the FBP images. The difference in visual impression gets obvious when subtracting the identical axial slice for the three reconstruction

Figure 4. Difference images for an axial slice (corresponding slice in Figure 1) through the liver: (a) PS-FBP, (b) PS-IR and (c) IR-FBP, image settings: window 69, level −990. Most notable differences between the reconstruction techniques are visible at the skin, bone structures (ribs, vertebrae) and in the surrounding air, in particular in comparison with PS. For homogeneous structures such as the liver, differences between IR and FBP images and between PS and FBP images. FBP, filtered back-projection; IR, iterative reconstruction; PS, PixelShine.

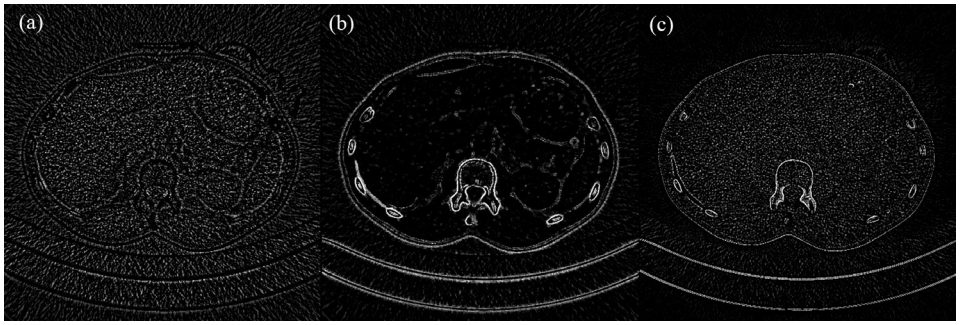

techniques (Figure 4). The stronger image noise is obvious when comparing PS- or IR-images with FBP-images, especially in the liver or spleen.

DISCUSSION

In this retrospective study, the influence of the post-processing algorithm PixelShine (AlgoMedica, Sunnyvale, CA) on the image characteristics (CT number and noise) and image quality in comparison to two standard CT reconstruction algorithms (FBP and IR) was investigated. For the purpose of this study, a low-dose protocol of the abdomen was assessed. Image noise is often pronounced in low-dose acquisitions so that differences in image noise can become obvious when altering the reconstruction process.

Objective image quality

IR is known to alter the textural features compared to FBP by means of a blotchy appearance or induced/increased artefacts.[11] PS claims to provide for CT images with exactly the same information as with FBP, however, while still reducing the image noise. Although significant differences in the CT numbers for the evaluated reconstruction methods were notable for the muscle and aorta, those differences were within 3 HU.

On average, CT numbers between the methods varied by less than 1 HU (maximum absolute difference of 3 HU for all evaluated patients and ROIs in the muscle). CT numbers provide a measure of a materials density and therefore link to its composition. In case of urinary stones, a shifted CT number might result in the assumption of the wrong genesis and affect the clinical diagnosis. Regarding the image noise, there were statistical significant differences between the reconstruction methods notable: employing PS on the FBP images reduced the image noise by up to 63% in the air and 48% in the soft tissues. Compared to IR, image noise was reduced by 15–27% in the soft tissues, 50% in the air and 6% in the aorta when using PS. Among the three reconstruction techniques, image noise was lowest for PS although the average CT numbers in the evaluated ROIs were not affected. Hence, calculated CNR and SNR values were highest for PS- and lowest for FBP-images throughout all ROIs. The reduction in image noise might allow for the reduction of the employed radiation exposure by 15–20%, while holding the image noise to the same level. The performed analysis on CT numbers did not show any notable differences in CT numbers, whereas the analysis on the image noise did. However, these traditional quantitative metrics do not represent the visual differences between difference reconstruction techniques.[11]

SNR, PSNR, RMSE and MAE describe how close a processed image is compared to a reference image. Since there is no ground-truth image available (such as a full-dose image), we chose to use the FBP images as reference. The analysis of the SNR, PSNR, RMSE and MAE has shown that IR images are closer to FBP images than PS processed images, since signal measures (SNR, PSNR) were higher and error measures (RMSE and MAE) were lower for IRs.

Subjective image quality

The image quality as rated by the two radiologists ranked between poor and moderate due to the low radiation exposure (average effective dose of 2.2 ± 1.4 mSv), c.f. Figure 3. Interrater-reliability was fair to moderate (0.40–0.49), due to the difference in experience (10 *vs* 2 years) and the stronger familiarization of rater 1 to images processed with PS. FBP images resulted in the lowest image quality (4.0 ± 0.8) for both raters, as they looked noisier than IR- or PS-processed images, especially in the liver (Figures 1 and 2). No differences in rated image quality were notable between IR-images and PS-processed images (Figure 3), although the image texture differed between the reconstruction methods (Figure 2).

Noise reduction techniques such as IR or PS cause a shift of the central frequency to a lower frequency, causing a texture change that is different for different technique.[16] Pan et al[16] compared PS to the reconstruction techniques ASiR (adaptive statistical iterative reconstruction) and ASiR-V from GE Halthcare (Waukeha, Wisconsin) and SAFIRE and ADMIRE of Siemens Healthineers (Forchheim, Germany). They concluded in their study that PS processed images lead to the least central frequency shift for the same amount of noise reduction or the most noise reduction for the same amount of central frequency shift.[16] These results show, that for the different evaluated reconstruction techniques, the smallest textural change is expected from PS for the same noise reduction. Other publications have not yet treated the structure sharpness and textural appearance in detail. Figure 4 shows image subtractions for an axial slice. Although there was a significant difference between CT numbers in the air when comparing IR and FBP images, the visual impression of the air in both cases looks similar. As was noted earlier, CT numbers and noise do not provide enough detail on the visual impression. Therefore, further analysis of the frequency distribution, noise power spectrum, SNR, PSNR, RMSE and MAE for the three reconstruction techniques is required.

Until now, there are only few publications on the software PS. Tian et al[17] performed Pixelshine on IR images (ASiR-VEO-FBP blending, GE Healthcare) of pelvic arterial phase CT. They concluded in their study that PS can improve the image quality, significantly reduce noise and improve the SNR and CNR. Our study confirms the positive influence on image noise, SNR and CNR for native phase abdominal CT examinations. Both mentioned research groups employ PS on IR images, which is contrary to our information of using PS with FBP images. The impact of the underlying reconstruction method for the in PS processed images needs to be assessed in a future study. Wisselink et al[18] employed PS on a COPDGene phantom images to assess the potential for dose reduction in lung emphysema densitometry. They used a variety of scan parameters and reconstruction techniques in combination with PS and demonstrated that PS can reduce image noise in low-density inserts of the phantom, especially in air and emphysema. Our study supports their findings with the highest noise reduction being determined in the air (up to 63% compared to FBP).

Costs and benefits

For this study, the evaluated software required FBP images from the CT scanner. On modern CT scanner installations, IR techniques are available and employed for most of the acquisitions. Using PS as a complement to IR increases the reconstruction time and image storage by a factor of approximately 3 since FBP images and further

processed images need to be created from raw data, in addition to the IR images. Furthermore, the number of reconstructed images included in the generation of a clinical diagnosis also increases. Therefore, PS might be implemented as reconstruction tool for individual CT protocols or as an alternative to IR techniques, ones the software is evaluated for more CT protocols and vendors. For existing CT scanner installations where no IR is available, PS could be implemented to either increase the image quality or reduce the employed radiation exposure.

Limitations

There was only a limited number of patients included in this study. This study needs to be extended to a larger study cohort and other body regions, such as the chest, for more thorough claims regarding the limitations and benefits of the evaluated software. Furthermore, only native acquisitions without contrast enhancement were included in this study. The influence of PS on the visibility of low-contrast lesions or small subtle-enhancing nodules has not been evaluated in detail yet. The CT examinations in this study were performed to visualize body packs with a large contrast, allowing for a non-contrast and low-dose protocol. Low-contrast lesions are difficult to visualize and evaluate in this setting. Here, all included patients had normal parenchymatous upper abdominal organs as far as visible from the low-dose non-enhanced images.

We did not give a comparison of the reader's detection performance on body packs for the included patients, since the packs were clearly identifiable on all images due to their size and density, independent of the reconstruction algorithm. This retrospective study was performed in this specific patient collective due to the employed low-dose CT protocol rather than the analysis whether foreign bodies are detectable. More methods exist to assess the image quality with regard to texture properties (*i.e.* blotchy or plastic-like impression) between the three evaluated techniques. However, we were primarily interested how the three reconstruction techniques influence the visual image quality and diagnostic performance.

Furthermore, this study did not evaluate the influence on the reconstruction type on image artifacts in particular. However, when judging the image quality by the radiologists, there was no difference on the strength or visibility of artifacts (*i.e.* streak artifacts, beam hardening) notable among the three evaluated reconstruction techniques. The defined settings PS is using for image reconstruction are not specified to reduce or influence the visibility of image artifacts. Therefore, a difference between the methods was not expected.

In this study, the standard PS software settings were used as suggested by the vendor for the specific CT scanner, reconstruction kernel and body region. More research on the impact of the settings on the image quality is necessary to validate the chosen parameter. Furthermore, since the number of DL methods for noise reduction is increasing, it would be of interest to compare the assessed DL method to other published DL methods.

REFERENCES

1. Mangold S, Wichmann JL, Schoepf UJ, Poole ZB, Canstein C, Varga-Szemes A, et al. Automated tube voltage selection for radiation dose and contrast medium reduction at coronary CT angiography using 3(rd) generation dual-source CT. *Eur Radiol* 2016; **26**: 3608–16. doi: https://doi.org/10.1007/s00330-015-4191-4
2. Greffier J, Frandon J, Pereira F, Hamard A, Beregi JP, Larbi A, et al. Optimization of radiation dose for CT detection of lytic and sclerotic bone lesions: a phantom study. *Eur Radiol* 2020; **30**: 1075–8. doi: https://doi.org/10.1007/s00330-019-06425-z
3. Lell MM, Kachelrieß M. Recent and upcoming technological developments in computed tomography. *Invest Radiol* 2020; **55**: 8–19. doi: https://doi.org/10.1097/RLI.0000000000000601
4. Geyer LL, Schoepf UJ, Meinel FG, Nance JW, Bastarrika G, Leipsic JA, et al. State of the art: iterative CT reconstruction techniques. *Radiology* 2015; **276**: 339–57. doi: https://doi.org/10.1148/radiol.2015132766
5. Stiller W. Basics of iterative reconstruction methods in computed tomography: a vendor-independent overview. *Eur J Radiol* 2018; **109**: 147–54. doi: https://doi.org/10.1016/j.ejrad.2018.10.025
6. May MS, Wüst W, Brand M, Stahl C, Allmendinger T, Schmidt B, et al. Dose reduction in abdominal computed tomography. *Invest Radiol* 2011; **46**: 465–70. doi: https://doi.org/10.1097/RLI.0b013e31821690a1
7. den Harder AM, Willemink MJ, de Ruiter QMB, Schilham AMR, Krestin GP, Leiner T, et al. Achievable dose reduction using iterative reconstruction for chest computed tomography: a systematic review. *Eur J Radiol* 2015; **84**: 2307–13. doi: https://doi.org/10.1016/j.ejrad.2015.07.011
8. Greffier J, Frandon J, Larbi A, Beregi JP, Pereira F. Ct iterative reconstruction algorithms: a task-based image quality assessment. *Eur Radiol* 2020; **30**: 487–500. doi: https://doi.org/10.1007/s00330-019-06359-6
9. Pontana F, Moureau D, Schmidt B, Duhamel A, Faivre J-B, Yasunaga K, et al. CT pulmonary angiogram with 60% dose reduction: Influence of iterative reconstructions on image quality. *Diagn Interv Imaging* 2015; **96**: 487–93. doi: https://doi.org/10.1016/j.diii.2014.08.006
10. van Osch JAC, Mouden M, van Dalen JA, Timmer JR, Reiffers S, Knollema S, et al. Influence of iterative image reconstruction on CT-based calcium score measurements. *Int J Cardiovasc Imaging* 2014; **30**: 961–7. doi: https://doi.org/10.1007/s10554-014-0409-9
11. Fletcher JG, Leng S, Yu L, McCollough CH. Dealing with uncertainty in CT images. *Radiology* 2016; **279**: 5–10. doi: https://doi.org/10.1148/radiol.2016152771
12. Kim JH, Yoon HJ, Lee E, Kim I, Cha YK, Bak SH. Validation of Deep-Learning image reconstruction for low-dose chest computed tomography scan: emphasis on image quality and noise. *Korean J Radiol* 2020; **21**: S5. doi: https://doi.org/10.3348/kjr.2020.0116
13. Akagi M, Nakamura Y, Higaki T, Narita K, Honda Y, Zhou J, et al. Deep learning reconstruction improves image quality of abdominal ultra-high-resolution CT. *Eur Radiol* 2019; **29**: 6163–71. doi: https://doi.org/10.1007/s00330-019-06170-3
14. Benz DC, Benetos G, Rampidis G, von Felten E, Bakula A, Sustar A, et al. Validation of

deep-learning image reconstruction for coronary computed tomography angiography: impact on noise, image quality and diagnostic accuracy. *J Cardiovasc Comput Tomogr* 2020; **14**: 444–51. doi: https://doi.org/10.1016/j.jcct.2020.01.002

15. Shin YJ, Chang W, Ye JC, Kang E, Oh DY, Lee YJ, et al. Low-Dose abdominal CT using a deep Learning-Based denoising algorithm: a comparison with CT reconstructed with filtered back projection or iterative reconstruction algorithm. *Korean J Radiol* 2020; **21**: 356. doi: https://doi.org/10.3348/kjr.2019.0413
16. Pan T, Hasegawa A, Luo D, Wu CC, Vikram R. Technical note: impact on central frequency and noise magnitude ratios by advanced CT image reconstruction techniques. *Med Phys* 2020; **47**: 480–7. doi: https://doi.org/10.1002/mp.13937
17. Tian S-F, Liu A-L, Liu J-H, Liu Y-J, Pan J-D. Potential value of the PixelShine deep learning algorithm for increasing quality of 70 kVp+ASiR-V reconstruction pelvic arterial phase CT images. *Jpn J Radiol* 2019; **37**: 186–90. doi: https://doi.org/10.1007/s11604-018-0798-0
18. Wisselink HJ, Pelgrim GJ, Rook M, van den Berge M, Slump K, Nagaraj Y, et al. Potential for dose reduction in CT emphysema densitometry with post-scan noise reduction: a phantom study. *Br J Radiol* 2020; **93**: 20181019. doi: https://doi.org/10.1259/bjr.20181019
19. den Harder AM, Willemink MJ, van Doormaal PJ, Wessels FJ, Lock MTWT, Schilham AMR, et al. Radiation dose reduction for CT assessment of urolithiasis using iterative reconstruction: a prospective intra-individual study. *Eur Radiol* 2018; **28**: 143–50. doi: https://doi.org/10.1007/s00330-017-4929-2
20. Sage D, Unser M. Teaching image-processing programming in Java. *IEEE Signal Process Mag* 2003; **20**: 43–52. doi: https://doi.org/10.1109/MSP.2003.1253553
21. Brennan RL, Prediger DJ. Coefficient kappa: some uses, misuses, and alternatives. *Educ Psychol Meas* 1981; **41**: 687–99. doi: https://doi.org/10.1177/001316448104100307
22. Huda W, Magill D, He W. Ct effective dose per dose length product using ICRP 103 weighting factors. *Med Phys* 2011; **38**: 1261–5. doi: https://doi.org/10.1118/1.3544350